京都大学防災研究所年報　第42号　B-1　平成11年4月
Annuals of Disas. Prev. Res. Inst., Kyoto Univ., No. 42 B-1, 1999

Modeling of Long-range Transport of Yellow-sand and Muddy Rain in East Asia

Zifa WANG　and　Hiromasa UEDA

Disaster Prevention Research Institute, Kyoto University, Kyoto 611, Japan

Abstract

A long-range transport model for yellow-sand is developed. A new module for mobilization process of yellow-sand is devised according to the analysis of observed mobilization data of meteorological stations in North China for ten years. The model considers the size spectrum of yellow-sand, the micro-physical process and the parameterization of dry and wet deposition in detail. For the model validation, the model results were compared with dust whirl reports of the synoptic weather code and with observed surface concentration at five stations in Japan for an intensive transport event of yellow-sand over East Asia in April 1988, showing a high degree of agreement. Then, by means of the present model, a heavy muddy rain in Beijing during April 15-16, 1998 is simulated successfully.

Keywords: Sand mobilization, long range transport, yellow-sand, air pollution model, deflation process

1. Introduction

The dust storm originated from the Asian continent in spring is a kind of destructively disastrous weather, which brings about tremendous loses to national economy and human life. Scientific interest in the chemistry and flux of the Asian dust has been stimulated for long time because the aeolian material plays an important role in the biogeochemical cycles of trace elements in the mid-latitude Northern Hemisphere (Uematsu et al. 1983, Preining 1991, Zhang 1994, and Niimuru 1997). The sandstorm from the Asia continent may have a path thousand kilometers long, and cover an area of 10^6-10^7km^2 (Murayama 1988), and the annual amount of airborne sand dust particles invades from 10^6 to 10^7 tons (Uematsu et al. 1983). Transport flux of dust particles from deserts and the Loess Plateau of China to Pacific Ocean is considered to be much larger than that from Sahara to Atlantic (Uematsu et al., 1983, Kotamarthi, et al. 1993), the relevant research is not enough to reveal the uncertainties about the yellow-sand transport. For example, when and how can the yellow-sand be blown up to the atmosphere and transported for a long distance? What kind of weather condition does the sandstorm come? To what amount is the dust flux to ocean areas attained for one transport process? In what way do the size distribution and chemical composition change during the long-range transport?

Many researches have been made on the meteorological conditions responsible for dust mobilization, loading and transport. Xu and Wu (1979) discussed the possible weather conditions causing a serious dust storm on April 22,1977. Uematsu et al. (1983) analyzed the dust storms

happened during the Asian history and Zhang (1984) estimated the amount of the dust deposition during the history of China by analysis its weather and climate conditions. Murayama (1988) provided the horizontal distribution of yellow-sand during 1982 to 1988, using GMS satellite data. Some observations for its size distribution, chemical components, vertical distribution and optical characteristics in North Pacific region show that the concentration of sulfur and nitric acid increase sharply during the yellow-sand transport process (Okada et al., 1990, Winchester and Wang, 1989).

Many models are used as a useful tool to afford a rough description of dust transport process in the atmosphere (Kotamarthi and Carmichael, 1993, Sheng and Qin, 1994, Liu and Zhou 1997), but the parameters used in the relevant mobilization module is simply copied from Sahara studies. To gain a detail temporal and spatial distribution of yellow-sand concentration in the atmosphere, it is necessary to develop Eulerian-type transport models that are able to represent all major relevant processes, especially the deflation process.

A heavy muddy rain was precipitated in Beijing during the 15-16,1998. The ground surface was covered a layer of dirty muddy mixed with polluted particles. It had much deeper influence on the citizen life than expected. Only to consider the fee to clean the cars would it be more than two million US dollars. In the paper, numerical studies have been carried out to evaluate the muddy rain that occurred around Beijing area during this period. For the purpose, a three-dimensional Eulerian long-range transport model for yellow-sand in East Asia has been developed based on a new parameterization for the dust uptake.

2. Model Description

The main phases which influence the temporal and spatial distribution of yellow-sand in the atmosphere are the deflation, advection, diffusion, dry deposition, wet deposition, chemical and micro-physical processes. In a spherical and terrain-following coordinate system, the yellow-sand concentration satisfies the mass conservation equation, which can be described mathematically by a system of partial differential equation of the form:

$$\begin{aligned}&\frac{\partial}{\partial t}(\Delta H\cdot C_i)+\frac{\partial}{R\cos\theta\partial\varphi}(u\cdot\Delta H\cdot C_i)+\frac{\partial}{R\cos\theta\partial\theta}(v\cos\theta\cdot\Delta H\cdot C_i)\\&+\frac{\partial}{\partial\sigma}(W\cdot C_i)=\frac{K_\varphi\partial}{R^2\cos^2\theta\partial\varphi}\left(\Delta H\cdot\frac{\partial C_i}{\partial\varphi}\right)+\frac{K_\theta\partial}{R^2\cos\theta\partial\theta}\left(\Delta H\cdot\cos\theta\frac{\partial C_i}{\partial\theta}\right)\\&+\frac{\partial}{\partial\sigma}\left(\frac{K_\sigma\partial C_i}{\Delta H\partial\sigma}\right)+Q\cdot\Delta H-D\cdot\Delta H-W_{ash}\cdot\Delta H+Micro\cdot\Delta H+Aqch\cdot\Delta H,\end{aligned}\quad(1)$$

where C_i(i=1,9) is the concentration of yellow-sand for i-th particle size range(size bin), t is the time, θ and φ are the latitude and longitude, R is the Earth radius, K_θ, K_φ, K_σ are the diffusion coefficients in different directions, u, v are the horizontal wind velocities, Q is the deflation rate of yellow-sand, D is the dry deposition parameter, W_{ash} is the in cloud and below cloud scavenging parameter, Micro is the parameter of micro-physical process, Aqch is the chemical transferring parameter. The terrain-following height coordinate σ can be written as,

$$\sigma(\theta,\varphi)=\frac{z-h(\theta,\varphi)}{H(\theta,\varphi)-h(\theta,\varphi)}=\frac{z-h}{\Delta H},\quad(2)$$

where H(θ,φ) is the height of the tropopause layer, h(θ,φ) is the height of relief, z is geopotential height. The equivalent vertical velocity W is computed using the mass continuity equation in terrain-following coordinate:

$$W=\omega-\frac{u}{R\cos\theta}\left(\frac{\partial h}{\partial\varphi}+\sigma\frac{\partial\Delta H}{\partial\varphi}\right)-\frac{v}{R}\left(\frac{\partial h}{\partial\theta}+\sigma\frac{\partial\Delta H}{\partial\theta}\right).\quad(3)$$

The boundary conditions used to solve equation (1) are set as these: yellow-sand can be promised to transport out of but not into the boundary. The bottom surface is assumed as an absorbing boundary while the top boundary as a closed one. The current model domain covers the East Asia from 16°N to 60°N, and from 75°E to 145°E with horizontal grids at 1°×1° resolution. The vertical extending consists of eight layers (σ=0.005, 0.025, 0.075, 0.15, 0.275, 0.45, 0.65, 0.875) from the surface to tropopause along a terrain-following height coordinate. A simplified but very accurate, mass conservative advection algorithm is used to solve the three-dimensional mass conservation equation (1) with a time-splitting technique (Walcek and Aleksic, 1998, Wang et al. 1997, Carmicheal et al. 1986). Greater stability of numerical solution is obtained while the Courant number (uΔt/Δx) is less than 1. Time step was chosen as 10 minutes. The algorithms of advection term and diffusion term are listed in the differential equation.

$$\frac{\Delta H(C^{n+1}-C)}{\Delta t}+\frac{1}{R\cos\theta}\frac{F_{i+1/2}-F_{i-1/2}}{\Delta\varphi}\frac{K_\varphi}{R^2\cos^2\theta_j}\frac{\Delta H_i(C_{i+1}-C_i)-\Delta H_{i-1}(C_i-C_{i-1})}{\Delta\varphi^2} \quad (4)$$
$$+\frac{F_{j+1/2}-F_{j-1/2}}{\Delta\theta}\frac{K_\theta}{R^2\cos\theta_j}\frac{\Delta H_j\cos\theta_j(C_{j+1}-C_j)-\Delta H_{j-1}\cos\theta_j(C_j-C_{j-1})}{\Delta\theta^2}$$
$$+\frac{F_k-F_{k-1}}{\Delta\sigma}-\left[\frac{K_\sigma}{\Delta H}\frac{(C_{k+1}-C_k)}{\Delta\sigma_k}+\frac{K_\sigma}{\Delta H}\frac{(C_k-C_{k-1})}{\Delta\sigma_{k-1}}\right]/\Delta\sigma_k$$
$$=Q\cdot\Delta H+D\cdot\Delta H-W_{ash}\cdot\Delta H+Micro\Delta H+Aqch\Delta H$$

where F is the flux at cell face which defined by introducing an "outflowing" mixing ratio Q_f (Walcek and Aleksic, 1998).

Yellow-sand particles are divided into nine bins (Table 1) from 0.5μm to 90μm in the model (Toon et al., 1988). In each of the size bins we distinguish three types of aerosols. The first type is not allowed to grow by depleting vapors, but can grow by coagulation. Examples of this type include yellow-sand, sea salt and carbon particles. The second type undergoes condensation growth such as water droplets and sulfuric acid aerosols. The final type is the mixture of the first two kinds. The size spectrum of yellow-sand depends on the deflation, gravitational settling, micro-physical processes in clouds and washout by precipitation.

Table 1 Classification of particles size and its meridian radius and representative gravitational settling velocity Vg (m/s) in the transport model of yellow-sand (unit of radius is μm)

bin	1	2	3	4	5	6	7	8	9
radiu	0.5	0.96	1.83	3.5	6.7	12.8	24.5	46.7	90.0
Vg	1.9×10^{-5}	4.01×10^{-5}	1.46×10^{-4}	5.34×10^{-4}	1.96×10^{-3}	7.15×10^{-3}	2.61×10^{-2}	9.57×10^{-2}	0.35

Dry deposition is a very important process in the life cycle of yellow-sand in the atmosphere. They influence directly the temporal and spatial distribution of yellow-sand and its long-range transport. Measurements of dry velocities in Chinese desert have been limited. Zhang et al. (1998) provided a simple way to reconstruct the dry deposition mechanism and calculated dry deposition velocities for 9 dust-derived elements during non-dust storm and dust storm periods. Following Zhang et al.(1998), deposition velocities of particles are calculated in this model by

$$V_d = V_g + u_*^2/(k\hat{u}(Sc^{0.6}+10^{-3/Stk})) \quad \text{for the lowest level of the model domain} \quad (5)$$

$$V_d = V_g \quad \text{for other model levels} \quad (6)$$

where u* is the wind friction velocity, $\hat{u}$ is the wind speed at the lowest level of the model, k is the von Karman's constant (=0.4), Sc is the particle Schmidt number, and S_{tk} is the particle Stokes number, which is a ratio of particle stopping distance to a length scale. V_g is the gravitational settling velocity and is determined for a particle with radius r using Stokes law

$$V_g = \frac{2\rho r^2}{9\gamma g} \quad (7)$$

where ρ is the particle density, g is the gravitational acceleration, and γ is the air viscosity. We obtained representative gravitational settling velocities for different bins of yellow-sand in the model, which were listed in Table 1.

The efficiency of aerosol removal by rain is usually described by the scavenging ratio Λ, which is calculated by (Pruppacher and Klett 1978),

$$\Lambda = 10.8\cdot E\cdot R^{0.16}/H \quad (8)$$

where E is the coagulation kernel (set as 0.83), R is the rainfall intensity ($mm.hr^{-1}$), and H is the depth of cloud or the model layer.

The role of micro-physical processes can be ignored under dry condition. However, most of long-range transport events of yellow-sand are accompanied with a frontal cyclone and precipitation. Sometimes muddy rain and yellow-snow may be observed. A sub-model to deal with the micro-physical processes of yellow-sand is developed and can be switched on in the transport model under suitable conditions. It considers coagulation, condensation, evaporation and washout by rain and can be written as (Prupacher and Klett 1978),

$$\frac{\partial C(v,t)}{\partial t}=\int_0^v K_c(u,v-u)C(u,t)C(v-u,t)du-C(v,t)\int_0^\infty K_c(u,v)C(u,v)du$$
$$-\frac{\partial C(v,t)g(v,t)}{\partial r}+S(v,t)+R(v,t)C(v,t), \quad (9)$$

where u,v represent particle volumes, Kc is the coagulation kernel, g(v,t) the condensation growth rate, r the particle radius, S the source term and R

the removal rate coefficient.

Input data include vegetation, topography, distribution of desert and loess plateau, size spectrum of dust in source areas and the threshold value of friction velocity for deflation. Meteorological fields are constructed using reanalysis data given from the ftp service (ftp://ftp.ncep.noaa.gov/) of the National Centers for Environmental Prediction (NCEP). The data are given at standard pressure levels of 1000, 925, 850,700, 600, 500, 400, 300 250, 200, 150 and 100hPa in the vertical. The meteorological parameters used in the model include horizontal wind, σ-wind, geopotential height, temperature and relative humidity. The interval of input is 6 hours. In the transport calculation the wind field at intermediate time steps is computed by linear interpolation of 6-h fields. The rainfall intensity used in the calculation is interpolated from the observation data of Meteorological Agency of China.

3. A new module for yellow-sand deflation

Deflation happens to occur under certain weather conditions. It is difficult to decide the threshold wind in the model because the critical values vary with processes and locations. Helgren and Prospers (1987) suggested that threshold velocity changed with soil type and location of stations and averaged value was 8.2m/s, varying from 5 to 12.5m/s, according to 41 dust blowing up processes happened at eight stations of Sahara during January and August 1974. Westphal et al. (1987) found the mean surface wind speed was 4.6m/s in 12 dust blowing up processes from Aug. 23 to Sept. 23, 1979 at the same eight stations. Kalma et al. (1988) showed that the threshold velocity for Australian dust storm was 6.5m/s at a level of 10m height. Murayama (1988) found the threshold velocity in loess plateau ranged from 10 to 12 m/s from the analysis of the relationship between the visibility and threshold velocity in loess plateau, outside and inside deserts in 1988 and 1989. Wind tunnel experiments (Hu and Qu 1997) provided the different threshold velocity and deflation rates of yellow-sand for the Gobi desert and the other desert, respectively. Westphal et al. (1987) adopted the critical friction velocity as a factor to judge whether the mobilization happened and calculated the amount of blowing up in Sahara region. Ina and Fung (1996) simulated emission, transport and optical height of dust particles in globe scale. They assumed desert, grassland and bare land as potential emission areas. Deflation amount was calculated from the surface wind speed and its threshold velocity. A mobilization module of Zhang (1994) applied in East Asia confined the potential emission regions in loess plateau (34~41°N, 102~114°E) and Gobi desert (40~45°N, 95~110°E) and considered two kinds of sources: continuous and point emissions.

Table 2 Weight factor (C_1) of dust loading for different land types

Landtype	water	broadleaf evergreen forest	mixed coniferous and broadleaf deciduous forest	high latitude deciduous forest	grassland	losses plateau
Weight factor	0	0	35	50	180	1200
Landtype	tundra	coniferous forest	broadleaf deciduous forest	shrubs and bare ground	cultivation	desert
Weight factor	0	30	40	240	200	1600

Our dust uptake parameterization module differs somewhat with other approaches (e.g., Westphal et al. 1988, Gillette and Passi 1988, Ina and Fung 1996). Most of modules used in East Asia only selected threshold velocity as criterion to determine deflation. The new module of yellow-sand mobilization is designed for East Asia, based on the detail analysis of meteorological condition, landforms and climate background by the dust whirl report at the synoptic weather code at about 300 meteorological stations in China. Most of dust deflation occurs in the area from 35° to 50°N in latitude and 90° to 110°E in longitude, where is coincided with the arid region and the Loess Plateau. The high frequency of dust mobilization in the area is due to its warm, dry weather and the strong wind caused by the channel effect of the Tibetan Plateau (Xuan 1997). According to the synoptic weather reports from 1980 to 1989 the mobilization is not limited to the Loess Plateau and desert areas but it can occur in most areas of North

China. So the potential source areas are divided into several distinctive types including deserts, the Loess Plateau, grassland, cultivated land and deciduous forest. The size distribution and weight factor of the dust load change with latitude and season for each landtype (Table 2). We assume that the process of particle blowing up into the atmosphere is realized in two steps.

First, dust can be mobilized on the ground only when the following conditions are satisfied.

1. Weather systems such as front and cyclone should be prevailing. Only when the potential source areas are controlled by these kinds of systems, will the deflation happen.

2. The friction velocity must overcome a threshold value. The threshold friction velocity changes with particle size, position and landtype and is obtained by the analysis of observation data of nearly 400 stations in North China.

3. The relative humidity at the lowest model level must also be lower than its critical value when mobilization happens.

Second, the amount of deflation is calculated as emission intensity of dust from the following equation

$$\frac{\Delta H_{i,j}\left(C^{t+1}_{i,j,l}-C^{t}_{i,j,l}\right)}{\tau}=\frac{Q_{i,j,l}}{\Delta\sigma_{i,j}} \qquad (10)$$

where $C^{t}_{i,j,l}$ is the concentration of yellow-sand of l-th bin at location i,j at time t, is the time step. ΔH, $\Delta\sigma$ are defined in equation (2). The emission intensity $Q_{i,j,l}$, which depends on kinematics condition at the lowest model level, is calculated by

$$Q_{i,j,l}=C_1C_2u_{*i,j,l}^{2}(1-u_{*0,i,j,l}/u_{*i,j,l})\cdot W_{i,j,l}\cdot R_{i,j,l} \qquad (11)$$

where the unit of $Q_{i,j,l}$ is kg/(m^2.s), C_1 is the weight factor for different landtype(Table 2), C_2 is a constant depending on experiments (Hu and Qu, 1997) and set as 2.9×10^{-11}, $u_{*i,j,l}$ is the kinematic friction velocity, $u_{*0i,j,l}$ is the threshold value of kinematics friction velocity and changes with landtype and location (Hu and Qu, 1997), $R_{i,j,l}$ is the fraction of l-th bin of deflating yellow-sand and is obtained from the spectrum distribution of dust in source areas. Table 3 and Table 4 show the size distributions of loess and desert soil particles at various locations (Liu 1986, Li 1987). $W_{i,j,l}$ is the humidity factor of landtype and calculated by

$$W_{i,j,l}=\begin{cases}(1-RH/RH_0) & for \quad RH<RH_0\\ 0 & for \quad RH\geq RH_0\end{cases}, \qquad (12)$$

where RH ,RH_0 are the relative humidity and its critical value at the lowest model level. The critical value was selected to be RH_0=40%。 The kinematics friction velocity is calculated by

$$u^{*}=\frac{V_s k}{[\ln\frac{z_s}{z_0}-\varphi(\frac{z_s}{L})]} \qquad (13)$$

where V_s is the wind at the lowest model level, k is the Karman constant, Z_0 is the roughness height, Z_s the height of the lowest model level, L the Monin-Obukhov length.

To test the above set of critical factors that were used to decide whether deflation happens in the module, the statistical results of dust deflation between observation and modeled are shown in Table 5 with different combination of these factors for April 1988. Test A used only the threshold value of kinematic friction velocity as a criterion to decide deflation. Test D is the approach in our new module. Tests B and C chose two factors. The total correct number increased from 7295 of Test A to 8582 of Test D and the total wrong number decreased from 2275 to 988. From the table we can see the threshold friction velocity is the most important but the other two factors could not be ignored. To consider all these factors gives much better result than that predicted by means of only one or two factors. If observed result shows 'deflation', the correct ratio of the prediction results of test D is lower than other tests and the ratio of 'fail to declare' is higher than other tests. If observed result shows 'no deflation', the false declaration ratio of test D is lower than other tests. If we use the sum of the total numbers of false declaration and fail to declare as criteria, test D is better than other tests.

Table 3 Size distributions (%) of loess particles at various locations

Radii (mm)	I	II	III	IV	V	VI	VII	VIII	IX	X	XI	XII	XIII	XIV
>0.1	0.5			4.5	6	3	2	3			2		2	
0.1-0.05	13.5	7	15	10.5	18	14	10.5	9	7	5	13	6	12	1
0.05-0.01	67	68	71	52	54	57	52	49	52	48	60	69.5	49	72

0.01-0.005	7.5	14	7	14.5	6	11	14.5	15.5	17	16.5	11	12	14	12
0.005-0.002	5.5	7	4	8	6	4	7.5	10.5	13	16	8	7.5	13	9
<0.002	5	4	3	10.5	10	11	13.5	13	11	14.5	6	5	10	6
mean	5.68	5.94	5.57	6.05	5.67	5.87	6.19	6.29	6.41	6.64	5.84	5.97	6.19	6.13

Note: I-Xining, Qinghai province, II-Qingyuan, III-Lanzhou, IV-Qingyang, Gansu province, V-Yulin, VI-Qingbian, VII-Luochuan, VIII-Changwu, IX-Wugong, X-Xian, Shannxi province, XI-Taiyuan, XII-Jixian, Shanxi province, XIII-Shanxian, XIV-Luoyang, Henan province.

Table 4 Size distributions (%) of potential desert land and desert at various locations

Radii (mm)	I	II	III	IV	i	ii	iii
1-0.25	7.39	2.97	4.19	2.53	15.89	24.19	36.27
0.25-0.05	72.17	92.15	67.72	87.27	67.88	37.57	49.56
0.05-0.01	12.22	3.56	19.09	6.45	12.24	20.66	10.06
0.01-0.005	1.04	0.47	0.75	0.13	0.38	3.73	1.43
0.005-0.001	2.68	0.07	2.36	1.15	0.84	6.05	1.57
<0.001	4.50	0.78	5.89	2.47	0.65	7.80	1.11

Note: I-potential desert land, II-developing desert land, III-severe developing desert land, IV-serious desert land, i-Kerxin desert, ii-east part of Erduoshi desert, iii-west part of Erduoshi desert.

Table 5 Statistics of dust deflation between observations and predictions according to different factors adopted in the model for April 1988

Type	observation	modeling	A	B	C	D
Correct	Deflation	Deflation	676	557	554	458
Fail to declare	Deflation	No	106	225	228	324
False declaration	No	Deflation	2169	1144	1336	664
Correct	No	No	6619	7644	7452	8124
Total correct			7295	8201	8006	8582
Total wrong			2275	1369	1564	988

where A、B、C、D are defined as

Condition	More than threshold value of kinematic friction velocity	More than critical relative humidity	Weather system judgment
A	Yes	No	No
B	Yes	Yes	No
C	Yes	No	Yes
D	Yes	Yes	Yes

4. Model validation

The yellow-sand transport episode over East Asia in April of year 1988 is chosen to test the model. Accompanying with two troughs of Europe moving eastward from April 9 to April 23, cold winds were blown up in Siberian and invaded into North China. As a result of high wind, dust storm, fly ash and floating dust covered Northwest, North and Northeast China for more than three times in a month. Floating dust reached to Yangtze River even extending to Guiling, a city in South China. The event was the most serious in these twenty years and characterized by its large scale and duration. The main transport processes are listed as following. Firstly, deflating from Taklimakan desert in April 9, the yellow-sand covered nearly all part of East Asia and transported from northwest to southeast, across Qinghai province, the Loess Plateau, North China, and reached South China and Japan. It disappeared in the southeast coastal in April 15. Secondly, it transported from north to south and arrived at the Center China from April 14 to 17. Then the yellow-sand changed its path from west to east. The third episode was an intensive deflation in the Loess Plateau in April 18. The ground-based observation data was collected to compare with simulation results.

Figure 1 shows the predicted patterns of dust concentration at the lowest model level, compared with observation from April 10 to April 21, 1988. Observed dust storm, fly ash and floating dust are denoted in the figures as weather report symbols in turn. They are observed in Taklimakan desert,

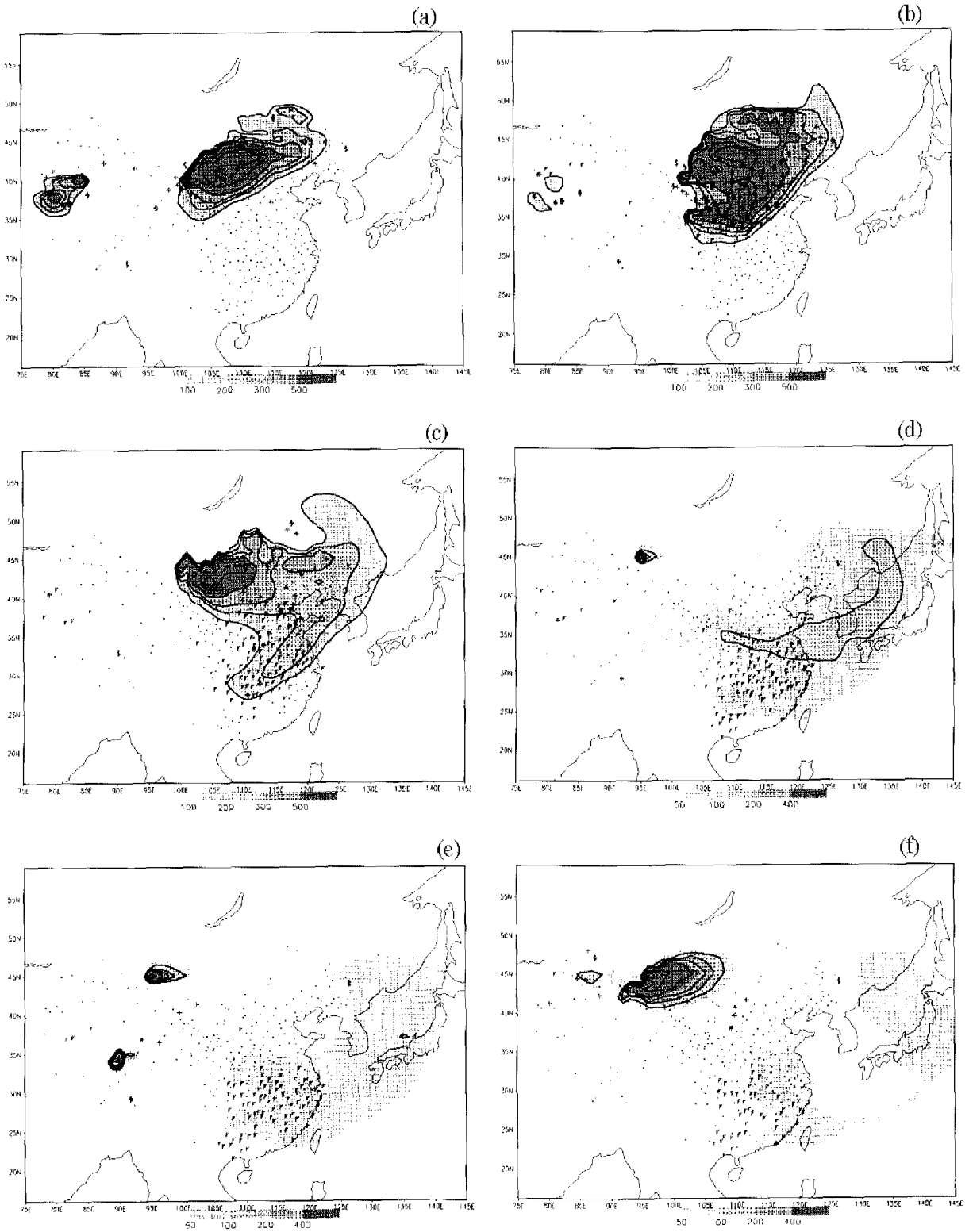

Fig. 1 Comparison of predicted (shaded contour) surface concentrations of yellow-sand and observation for (a) April 10, (b) April 11, (c) April 12, (d) April 13, (e) April 14, (f) April 15, (g) April 16, (h) April 17, (i) April 18, (j) April 19, (k) April 20, and (l) April 21. Marks denote floating dust storm, fly ash storm and dust storm, respectively, listed up in the dust whirl reports. The dots represent weather stations.

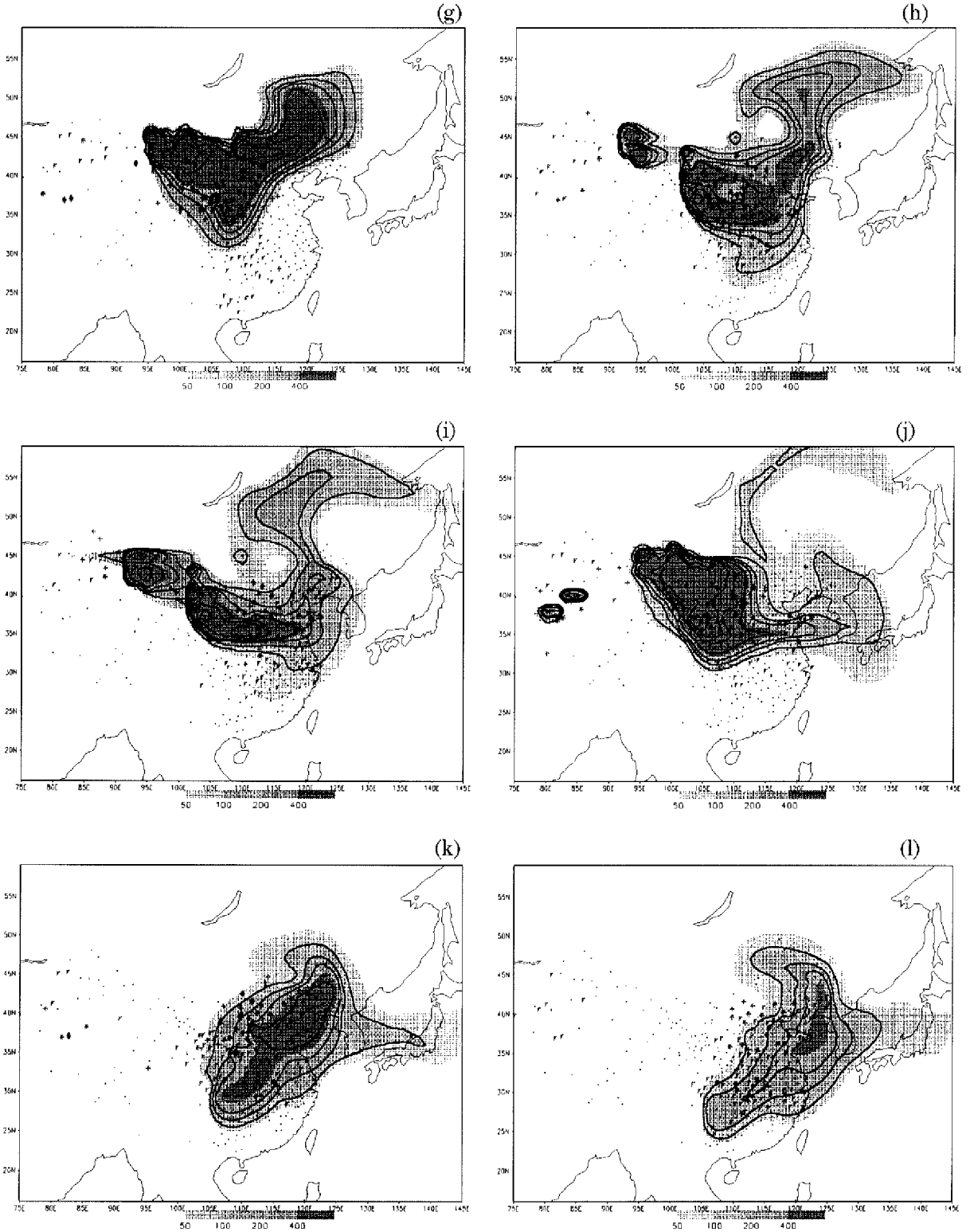

Fig.1 *(continued)*

Mongolia, Inner Mongolia, Gansu and Shannxi provinces on April 10. Calculated surface high concentration also appeared in those areas with maximum value 1500 $\mu g/m^3$ (Fig. 1(a)). Then yellow-sand transported toward southeast and covered Northeast, North and East China, reaching eastward to the coastal area such as Bohai Sea and southward to Central China on April 11. The observed distribution shows a good agreement with calculated area except for the false of predicting the dust storm in the Taklimakan desert (Fig. 1(b)).

The predicted yellow-sand concentration decreased continuously and transported eastward to Korea peninsula and southward to 25°N on April 12. Nearly all of the stations in the east part of China were observed floating dust with an excellent agreement with calculation (Fig. 1(c)). No new dust storm happened on April 12 and 13. The floating dust was predicted to be disappeared in source areas and North China. It transported southward to Taiwan and eastward to western Japan, mainly covering the East and South China, the East China Sea, and the Huanghai Sea, the Bohai Sea and Korea peninsula. Observed floating dust was located mainly in South China, having a similar shape with calculation (Fig. 1(d)).

The predicted high concentration of yellow-sand is located in two regions on April 14. One is a new deflation area of dust from 40° to 48°N and from 85° to 100°E, the other is the floating dust with much more decreased concentration, remaining from the day before and covering South China, East China and whole Japan (Fig. 1(e)). Observed yellow-sand distribution agrees with the prediction quite well. For these two days comparison with the observed surface yellow-sand concentration in some sites of Japan will be made in the next subsection 4.3. On April 15 there are three high concentration areas (Fig. 1(f)). The western part is a developing dust storm with much higher concentration while the other two are disappearing.

Another deflation had been developing intensively in Northwest China on April 16 with the concentration more than 1500$\mu g/m^3$ in source area (Fig. 1(g)). It transported very quickly from north to south and it covered North China and Central China within one day. Observed dust storms concentrated on the Loess Plateau and floating dusts had already arrived at Central China (Fig. 1(g)). The floating dust continued to move to south, reaching eastward to Shandong peninsula and southward to Hunan province on April 17 (Fig. 1(h)). Predicted yellow-sand concentration reached northward to Siberian although no corresponding data being available.

Figure 1(i) shows a transport path from northwest to southeast on April 18. High concentration was located along 35°N from 100° to 115°E, with values more than 1500$\mu g/m^3$ in some areas. The floating dust reached to Korea peninsula in east and to Zhejiang and Jiangxi provinces in south. The observed data supports the prediction. It transported eastward to western Japan on April 19 (Fig. 1(j)). There was no new deflation, and only floating dust existed on April 20 and 21, covering nearly whole part of the Pacific Rim regions (Fig. 1(k) and 1(l)). Observation shows a good agreement with prediction in both shape and intensity in these days.

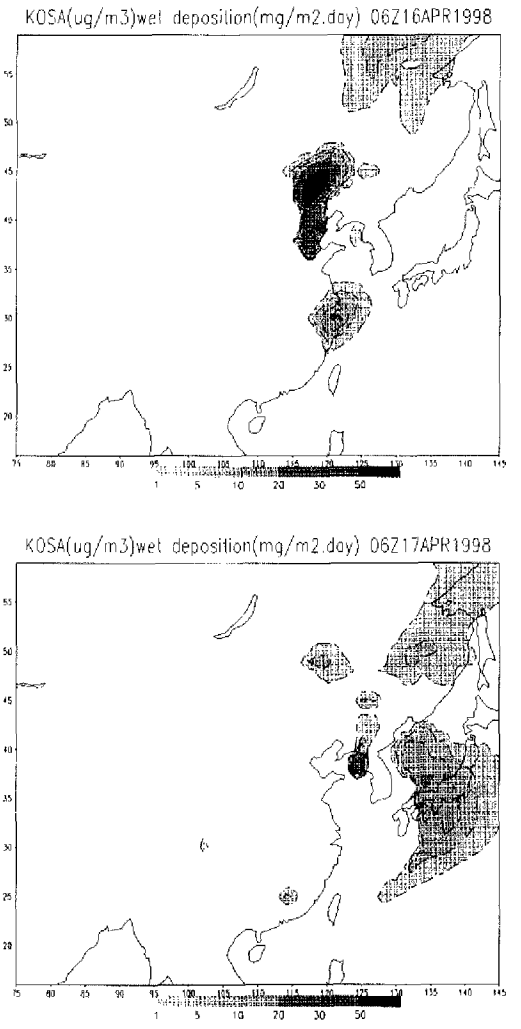

Figure 2 Predicted wet deposition of yellow-sand on April 16 and 17,1998.

5. Muddy rain simulation and discussion

Fig.2 shows the predicted wet deposition amount of yellow-sand on April 16 and 17, 1998. It is on that day heavy muddy rain was observed in Beijing. The model results predict it well. On April 16 and 17 relative higher concentrations of aerosols are also observed in Shanghai city. The simulation results about the long-range transport processes of yellow-sand especially the formation of muddy rain have been compared with satellite cloud picture and surface observation, showing a high degree of agreement. The cloud physics and precipitation process mixed with plenteous of yellow-sand from loess plateau, especially the size less than 2μm, led to the heavy muddy rain in North China.

References

Gillette, D.A and Passi, R. (1988): Modeling dust emission caused by wind erosion, *J. Geophys. Res.*, *93*, 14233-14242..

Helgren, D.M. and Prosepers, J.M. (1987): Wind velocities associated with dust deflation events in the western Sahara, *J.Climate Appl. Meteor.*, *26*, 1147-1151.

Hu, M.C. and Qu, J.Z. (1997): Preliminary estimate of dust deflation amount in Hexi Corridor, Gansu province, *Dust Storm Studies in China*, 118-120, Chinese Meteorological Press, Beijing.

Ina, T. and Fung, I. (1996): Modeling of mineral dust in the atmosphere, source, transport and optical thickness, *J. Geophy. Res.*, *101*, 14428-14439.

Joussaume,S. (!990): Three-dimensional simulations of the atmospheric cycle of desert dust particles using a general circulation model, *J.Geophys. Res.*, *95*,1909-1941.

Kalma, J.D., Speight, J.G. and Wasson, R.J. (1988): Potential wind erosion in Australia, A continet al. perspective, *J.Atmos. Sci.*,*8*, 411~428.

Kotamarthi, V.R. and Carmichael, G.R. (1993): A Modeling Study of the Long Range Transport of Kosa using Particle Trajectory Methods, *Tellus*, *45B*, 426-441.

Li Z. (1987): *Chinese Deserts*, p87-110, Academic Press, Beijing.

Liu D. (1986): *Loess and Environment*, p182-220, Academic Press, Beijing.

Liu Y. and Zhou, M.Y. (1997): A numerical simulation of dust storm and its long range transport process, *Journal of Nanjing Institute of Meteorology*, 20, 511-517.

Murayama, N. (1988): Dust cloud "Kosa" from the east Asian dust storms in 1982-1988 as observed by the GMS satellite. *Met. Sat. Center Tech Note*, *17*, 1-8.

Nickovic, S. and Dobricic, S. (1996): A model for long-range transport of desert dust, *Mon. Wea. Rev.*, *124*, 2337-2345.

Niimura, N. (1997): Analytical Study on the Atmospheric Transport Dust-Storm Particles in East Asia, Doctoral dissertation of University of Tsukuba.

Okada, K., Naruse, H. and Tanaka, T. (1990): X-ray spectrometry of individual Asia dust-storm particles over the Japanese islands and the North Pacific ocean, *Atmos. Environ.*, *24A*, 1369-1378.

Preining, O. (1978): Aerosol and Climate: An Overview, *Atmos. Environ.*, **25A**(11), 2443-2454.

Pruppacher H.R. and Klett, J.D. (1978): *Microphysics of Cloud and precipitation*, 714-724, Reidel.

Sheng, P.X and Qin, Y. (1994): Trajectory analysis for the dust storms over China, Proceedings of 4th international conference on Atmospheric Sciences and Applications to Air Quality, Seoul, Korea, pp. 200.

Toon, O.B., Turco, R.P., Westphal, D., Malone, R. and Liu, M.S. (1988): A multidimensional model for aerosols, description of computational analogs, *J. Atmos. Sci*, *45(15)*, 2123-2143.

Uematsu, M., Duce, R.A., Prospero, J.M., Chen, L., Merrill, J.T. and McDonald, R.L. (1983): Transport of Mineral Aerosol from Asia over the North Pacific Ocean, *Journal of Geophys. Res.*, *88(C9)*, 5343-5352.

Wang Z., Huang, M., He, D., Xu, H. and Zhou, L. (1997): Studies on transport of acid substance in China and East Asia Part I: 3-D Eulerian transport model for pollutants, *Scientia Atmospherica Sinica*, **21(3)**,366-378.

Welcek. C. J. and Aleksic, N.M. (1998): A simple but accurate mass conservative peak-preserving, mixing ratio bounded advection algorithm with Fortran code, *Amtos. Environ.*, *32*, 3863-3880.

Westphal D., Toon, O.B. and Carlson, T.N. (1987): A two-dimensional numerical investigation of the dynamics and microphysics of Saharan dust storms, *J. Geophys. Res*, *92*, 3027-3049.

Winchester, J.W, and Wang, M.X. (1989): Acid-base balance in aerosol components of Asia-Pacific region, *Tellus, 41B*, 323-337.

Xu, G.C. and Wu, G.X. (1979): Analysis of the "4.22" dust storm in Gansu province, *Acta Meteor. Sinica, 37(4)*, 26-35.

Xuan, J. (1997): Determining factors of dust emission rate in natural environment. *Proceedings of 1st international workshop on monitoring prediction of acid rain*, pp.13-28, Seoul, Korea.

Yang, D.Zh.. (1991): A transport process of yellow-sand, *Acta Meteor. Sinica,49*,334-342.

Zhang X. Y., Akimoto, R., Zhu, G.H., Chen, T. and Zhang, G.Y. (1998): Concentration, size distribution and deposition of mineral aerosol over Chinese desert regions, *Tellus, 50B*, 317-330.

Zhang Y. (1994): The Chemical Role of Mineral Aerosols in the Troposphere in East Asia, Doctoral dissertation of the University of Iowa.

要　旨

黄砂の長距離輸送モデルを開発した。数値モデルでは、10 年間にわたる北部中国の飛散観測の気象台データの解析から得られた、黄砂の飛散プロセスの新しいモジュールを導入し、黄砂の粒径分布、微物理過程、乾性沈着、湿性沈着過程を詳細に記述したものである。数値モデルの検証のために、モデル結果は、1988 年 4 月の東アジアでの黄砂大襲来時の中国の粉塵飛散報告や日本の５つの常時監視局の地上観測濃度と比較され、良い一致を見ている。この数値モデルを用いて、1998 年 4 月 15-16 日北京で発生した泥雨のシミュレーションを行った。

キーワード：砂塵流動、長距離輸送、黄砂、大気汚染モデル、再飛散プロセス